

Electronic Supplementary Information

A facile approach to superhydrophobic and superoleophilic graphene/polymer aerogels

Run Li, Caibao Chen, Jing Li, Liming Xu, Guyu Xiao*, and Deyue Yan

School of Chemistry and Chemical Engineering, State Key Laboratory of Metal Matrix Composites, Shanghai Jiao Tong University, 800 Dongchuan Road, Shanghai 200240, P. R. China

1. The optimization of preparation conditions

The reaction conditions such as the temperature, the time, the weight ratio of GO/PVDF and the volume ratio of DMF to deionized water were optimized to achieve the superhydrophobic aerogels. As shown in Table S1, when the temperature

Table S1. Contact angle of the graphene/PVDF aerogels under various preparation conditions.

Entry	Temperature (°C)	Time (h)	GO/PVDF ^a (mg/mg)	DMF/water ^b (mL/mL)	Contact Angle (degree)
1	160	10	20/50	8/2	152.9
2	150	10	20/50	8/2	– ^c
1	160	10	20/50	8/2	152.9
3	160	15	20/50	8/2	153.1
4	160	10	20/8	8/2	141.2
5	160	10	20/20	8/2	140.9
1	160	10	20/50	8/2	152.9
6	160	10	20/100	8/2	– ^d
7	160	10	20/50	6/4	– ^e
8	160	10	20/50	7/3	153.6
1	160	10	20/50	8/2	152.9
9	160	10	20/50	9/1	149.0

^a The weight ratio of GO/PVDF (20 mg GO). ^b The volume ratio of DMF/water (10 mL in total).

^c The gel was composed of several pieces. ^{d,e} Many sediments were observed except for the gel.

was 150 °C (*entry 2*), the product was not a monolith gel, which was made up of several pieces probably due to the incomplete reduction. In contrast, the mixed dispersion of GO and PVDF formed a monolith gel at 160 °C and its corresponding aerogel showed a contact angle of 152.9°. Subsequently, the effect of reaction time on the contact angle was investigated. At 160 °C, a further increased reaction time only

* Corresponding author. Tel: +86 21 54742664, E-mail: gyxiao@sjtu.edu.cn

slightly enhanced the contact angle as the reaction time was longer than 10 h (*entry 1 and 3*). However, the ratio of GO/PVDF greatly affected the contact angle of the resulting aerogels. When the weight ratio of GO/PVDF was 20/8 or 20/20 (*entry 4 and 5*), the contact angle of resulting aerogels was $\sim 141^\circ$. Contrastingly, the contact angle of the resulting aerogel was 152.9° as the weight ratio of GO/PVDF was decreased to 20/50. Unfortunately, the product showed some sediments except for the gel as the weight ratio of GO/PVDF was further reduced to 20/100 (*entry 6*) because the enhanced PVDF component could not well dissolve in the mixture of DMF and deionized water. On the other hand, PVDF is soluble in DMF but not soluble in water, whereas GO could disperse in water but not very well in DMF, so the ratio of DMF to water is significant for the preparation of the graphene/PVDF aerogels. For example, many sediments were observed except for the gel when the volume ratio of DMF/water was 6/4 (*entry 7*). This might be because the limited DMF in the mixed solvent deteriorated the dissolution of PVDF under the solvothermal conditions. When the volume ratio of DMF/water was increased to 7/3 or 8/2, the monolith gels were achieved and the contact angle of the resulting aerogels was higher than 150° (*entry 8 and 1*). Nevertheless, the contact angle of the as-made aerogel was lower than 150° as the volume ratio of DMF/water was further increased to 9/1 (*entry 9*). Therefore, the optimal reaction conditions were as follows: 160°C , 10 h, GO/PVDF = 2/5, and DMF/water = 7/3 or 8/2.

Fig. S1. Optical images of a water droplet on the surface of pure graphene aerogels (**a**: the graphene prepared in DMF/water (volume ratio = 7/3), the contact angle is 85.5° ; **b**: the graphene prepared in DMF/water (volume ratio = 8/2), the contact angle is 97.2°).

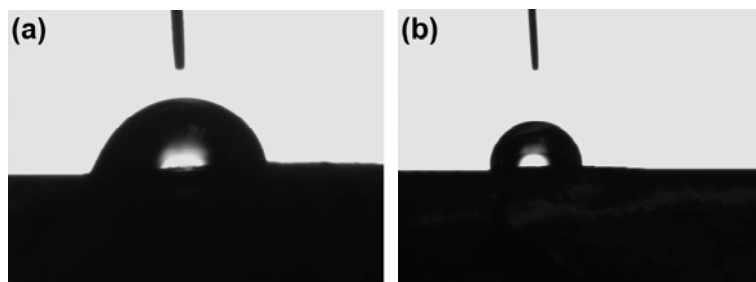


Fig. S2. SEM images of white PVDF particles (micro-size) on AG-1 (a) and AG-2 (b).

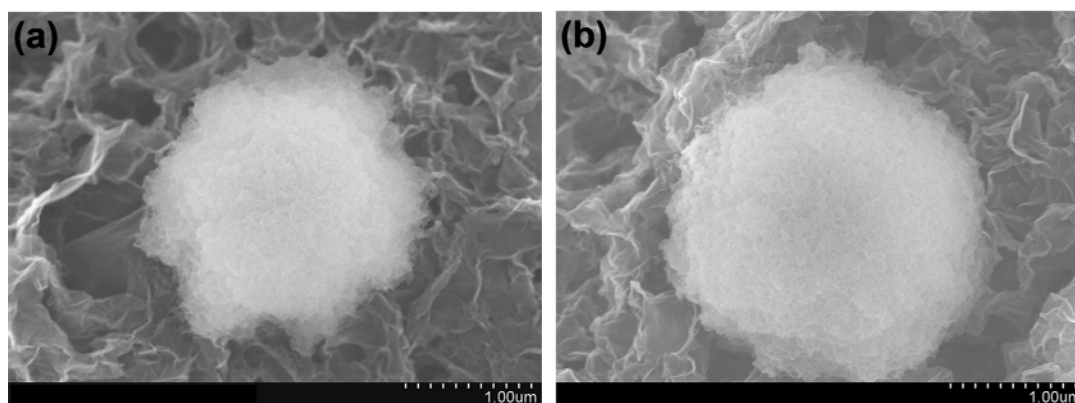


Fig. S3. Diameter distribution of the PVDF nanoparticles on the surface of AG-1 and AG-2 (statistic data from an area of $85 \times 85 \text{ nm}^2$).

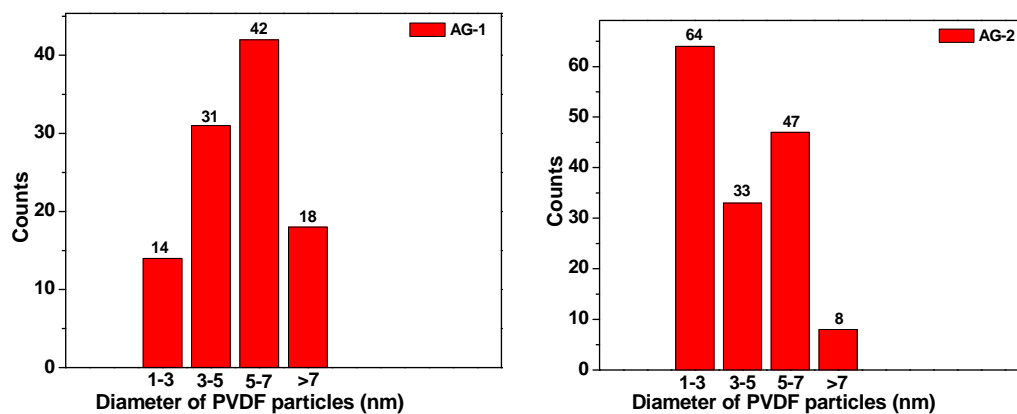


Fig. S4. SEM images of AG-1 (a) and AG-2 (b) treated under vacuum at 180°C for 10 hours.

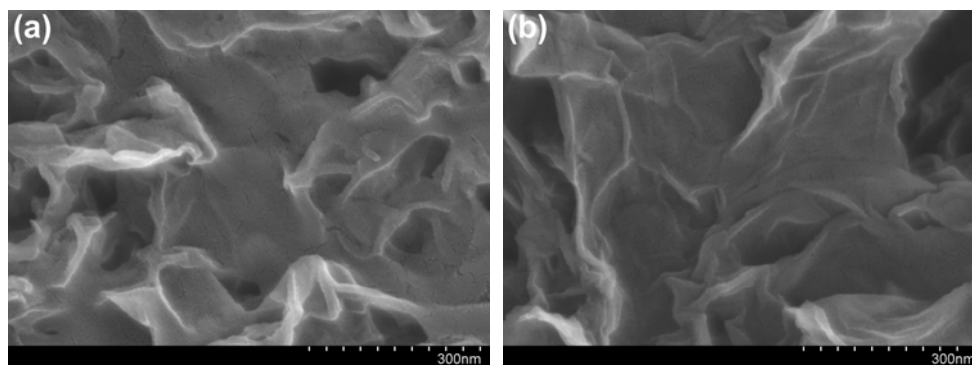


Fig. S5. Video snapshots of the absorption process of a drop of dodecane on the surface of AG-1 (a) and AG-2 (b)

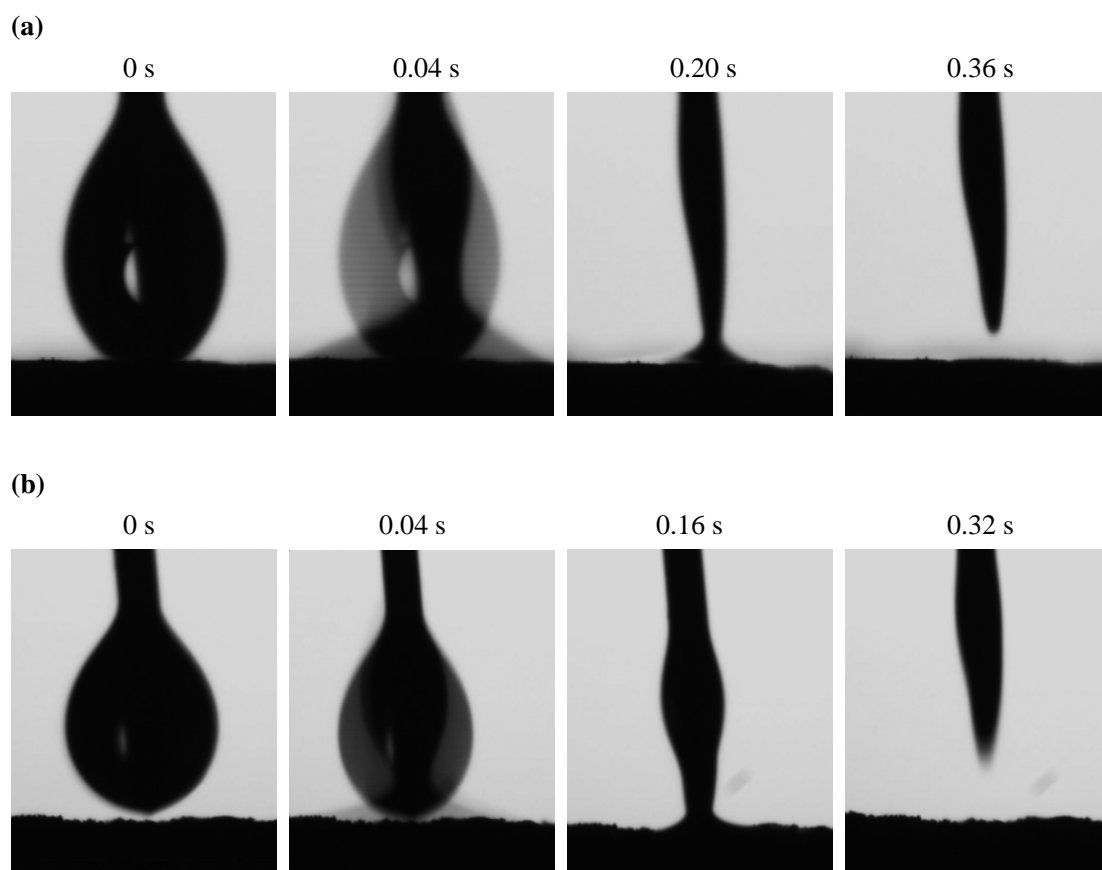


Fig. S6. Optical images of AG-2 immersed in water by an external force.

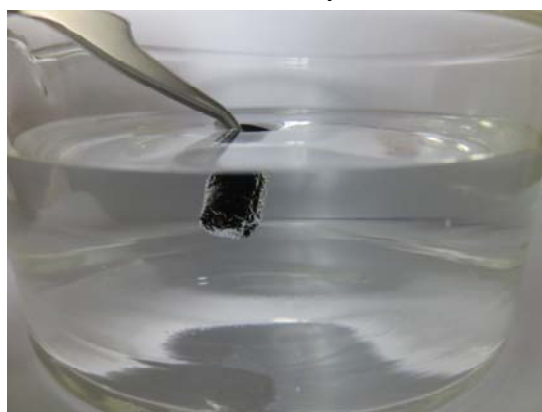


Fig. S7. FT-IR spectra of three kinds of the recovered oils from AG-1 (a) and AG-2 (b).

